

Instanton filtering for the stochastic Burgers equation

Tobias Grafke,¹ Rainer Grauer,¹ and Tobias Schäfer²

¹*Theoretische Physik I, Ruhr-Universität Bochum,
Universitätsstr. 150, D44780 Bochum (Germany)*

²*Department of Mathematics, College of Staten Island, CUNY, USA
(Dated: August 9, 2018)*

We address the question whether one can identify instantons in direct numerical simulations of the stochastically driven Burgers equation. For this purpose, we first solve the instanton equations using the Chernykh-Stepanov method [Phys. Rev. E **64**, 026306 (2001)]. These results are then compared to direct numerical simulations by introducing a filtering technique to extract prescribed rare events from massive data sets of realizations. Using this approach we can extract the entire time history of the instanton evolution which allows us to identify the different phases predicted by the direct method of Chernykh and Stepanov with remarkable agreement.

PACS numbers: 47.27.Ak, 47.27.E-, 47.27.ef, 05.40.-a

Introduction Understanding intermittency in turbulent flows is still one of the open problems in classical physics. More than 15 years ago, for certain systems like the problem of passive advection and Burgers turbulence the door for attacking this issue was opened by getting access to the probability density function to rare and strong fluctuations by the instanton approach [1–4]. In this letter we concentrate on rare fluctuations in Burgers turbulence. For that case, Gurarie and Migdal [2] introduced the instanton approach and were able to calculate the instanton contribution to the right tail of the velocity increment probability distribution function (PDF). In succeeding work, Balkovsky et al. [4] were able to characterize the left tail of the increment PDF making use of the Cole-Hopf transformation [5, 6]. These analytical results were confirmed by direct numerical solution of the instanton equations by Chernykh and Stepanov [7].

The open question remained whether one can observe or identify the instanton in numerical simulations of the stochastic Burgers equation. The answer is not obvious, since one could argue that, perhaps, the contribution of the instanton is exponentially small such that instantons are only relevant to such rare events that they are not interesting from a practical point of view at finite Reynolds numbers. In this Letter, however, we find that already at moderate Reynolds numbers the instanton can be identified in data sets of simulations of the stochastic Burgers equation. This gives a positive answer to this important question. In particular, we show by introducing a particular filtering technique that all phases of the instanton evolution can be recovered from data sets of simulations of the stochastic Burgers equation.

The Letter is organized as follows: we first review the path integral formulation for Burgers turbulence and revisit the algorithm introduced by Chernykh and Stepanov to solve directly the instanton equations. We then describe our numerical simulations to obtain sufficient statistical data ($\approx 10^7$ realizations of complete stochastic Burgers simulations using CUDA graphics

cards) necessary for our instanton filtering. Using this enormous data set we apply our instanton filtering procedure and compare the results with the direct instanton simulations. A conclusion and outlook summarize the Letter.

Action functional and instanton equations. We consider the stochastically driven Burgers equation given by

$$u_t + uu_x - \nu u_{xx} = \phi \quad (1)$$

with a noise field ϕ that is δ -correlated in time and has finite correlation in space with correlation length L , more precisely

$$\langle \phi(x, t) \phi(x', t') \rangle = \delta(t - t') \chi((x - x')/L), \quad (2)$$

$$\chi(x) = (1 - x^2) e^{-x^2/2}. \quad (3)$$

While the precise form of χ is not important for the results of our work, we chose this particular form in order to have the same setup of the problem as in previous studies by Chernykh and Stepanov. Using the functional path integral introduced by Martin-Siggia-Rose/Janssen-de Dominicis [8–11], the PDF of the velocity gradients $u_x(t = 0, x = 0)$ is written as

$$\mathcal{P}(a) = \int \mathcal{D}u \mathcal{D}p \mathcal{D}\mathcal{F} \exp\left(-\tilde{S}(u, p, \mathcal{F})\right), \quad (4)$$

with the action \tilde{S} given by

$$\begin{aligned} \tilde{S} = & \frac{1}{2} \int_{-\infty}^0 dt \int dx_1 dx_2 p(x_1, t) \chi(x_1 - x_2) p(x_2, t) \\ & - i \int_{-\infty}^0 dt \int dx p(u_t + uu_x - \nu u_{xx}) \\ & - 4\nu^2 \mathcal{F}i(u_x(0, 0) - a), \end{aligned} \quad (5)$$

where \mathcal{F} results from the Fourier transform of the δ -function for the observable $u_x(t = 0, x = 0) = a$. The saddle point (instanton) equations for the fields (u, p)

yielding the largest contribution to the path integral for strong gradients are then given by

$$u_t + uu_x - \nu u_{xx} = -i \int \chi(x - x') p(x', t) dx' \quad (6a)$$

$$p_t + up_x + \nu p_{xx} = 4i\nu^2 \mathcal{F}\delta(t)\delta'(x) . \quad (6b)$$

The Chernykh-Stepanov algorithm revisited. The algorithm proposed by Chernykh and Stepanov for solving the system of partial differential equations for the fields u and p can be summarized as follows: the diffusion terms in the equations (6) define the temporal direction of the numerical integration of the equations, meaning that u is integrated forward in time while p is integrated backwards. The right-hand side of equation (6b) poses the initial condition $p(t = 0, x) = -4i\nu^2 \mathcal{F}\delta'(x)$ and the starting step is obtained by setting $u(t, x) = 0$. Equation (6b) is then solved backward in time up to a large negative time mimicking $-\infty$. The obtained solution $p(t, x)$ is used in the right-hand side of equation (6a) such that this equation can be solved forward in time. This procedure is then iterated until convergence. For higher gradients, a stabilization of this iteration has to be applied, details of which can be found in [7]. While Chernykh and Stepanov use a stabilized finite difference scheme with an implicit first-order time integration, we utilize a second-order Adams-Bashforth temporal integration for a pseudo-spectral method. We also note the similarity of the system (6) to equations that arise in the context of transition probabilities [12, 13]. Although the boundary conditions are different, the above system of instanton equations can, in principle, also be solved numerically by minimizing the corresponding action using a L-BFGS scheme. We found, however, for the case under consideration, the propagation-based Chernykh-Stepanov scheme numerically much more efficient. Therefore, the Chernykh-Stepanov scheme might be an interesting alternative to compute transition probabilities. A detailed comparison of both schemes is beyond the particular scope of this paper and will be presented elsewhere.

Parallel simulation of the stochastic Burgers equation. In order to generate data from simulations of the stochastic Burgers equation, we need to solve eq. (1) with the appropriate right-hand side. For the generation of the stochastic force field ϕ , at each step in time, we draw a vector r of appropriately scaled normally distributed random numbers. The size of the vector corresponds to the discretization in x . This vector r is then multiplied by a matrix A resulting from the Cholesky decomposition of the (discretized) correlation matrix C . Note that naive discretization of χ may lead to a \tilde{C} that, due to finite machine-precision, is not positive-semidefinite. Therefore we used the algorithm introduced in [14] in order to obtain a matrix C that is positive-semidefinite and sufficiently close to \tilde{C} . Note that this method of generating

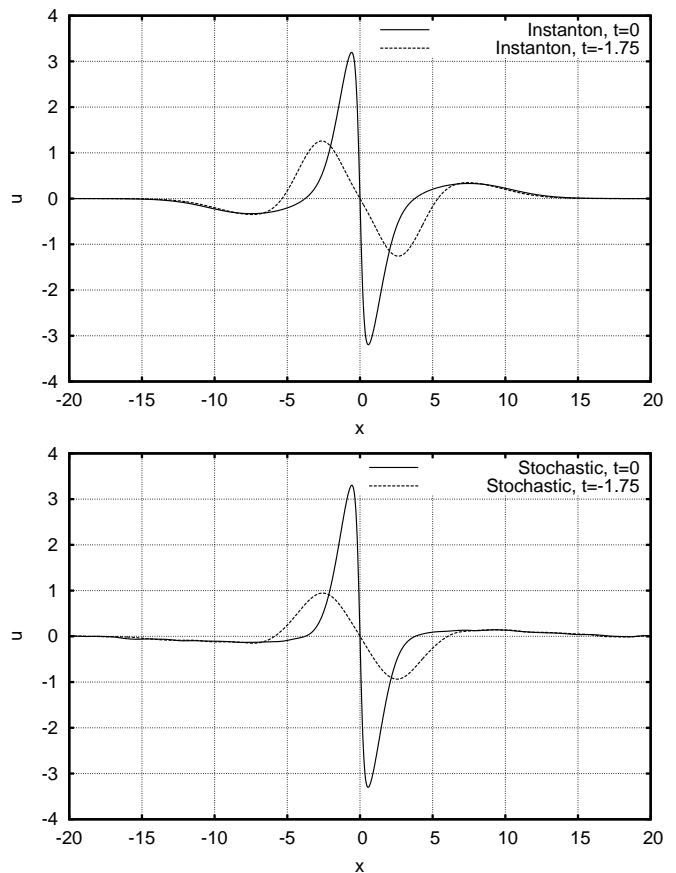


FIG. 1: Comparison of the filtered velocity field $\langle u_{\text{shifted}}(t, x) \rangle$ (top) and the instanton field $u(t, x)$ (bottom) at times $t = 0$ (solid) and $t = -1.75$ (dashed).

the noise term in eq. (1) is different from Fourier-based methods that are commonly used for such simulations [15, 16] and more computationally expensive. The reason for the presented choice was motivated by the necessity to numerically generate noise that closely imitates the fluctuations assumed in the instanton analysis.

As the size of an individual realization is small enough to fit on a single graphics card with its complete history, the whole simulation is performed in CUDA alone. Matrix-Vector-operations are realized using the cuBLAS-package, the fast Fourier-transform is provided by cuFFT. Since the filtering and shifting procedure was also implemented in CUDA, a whole bulk of simulations is performed and filtered independently on the GPU. Averaging over different CUDA-processes occurs after completion of a bulk and is performed via MPI. Thus, both expensive device-to-host copies and high-latency network communication are minimized. Because of the stochastic independence of realizations, this method scales linearly with the number of graphics cards.

Extracting the instanton. In order to provide a sufficient data set for the extraction of the instanton from simu-

	N	dx	η	L	L_{box}	ν	ϵ_k	T_L	#hits (%)
Run 1	1024	0.039	0.406	1	40	0.3	4.586	0.99	10.5
Run 2	1024	0.039	0.464	1	40	0.38	2.691	0.97	0.410
Run 3	1024	0.039	0.481	1	40	0.41	2.33	0.95	0.052

TABLE I: Parameters of the numerical simulations. N : number of collocation points, dx : grid-spacing, $\eta = (\nu^3/\epsilon_k)^{1/4}$: Kolmogorov dissipation length scale, L : correlation length of forcing, L_{box} : domain length, ν : kinematic viscosity, ϵ_k : mean kinetic energy dissipation rate, $T_L = L/u_{\text{rms}}$: large-eddy turnover time, #hits (%): percentage of hits with prescribed velocity derivative.

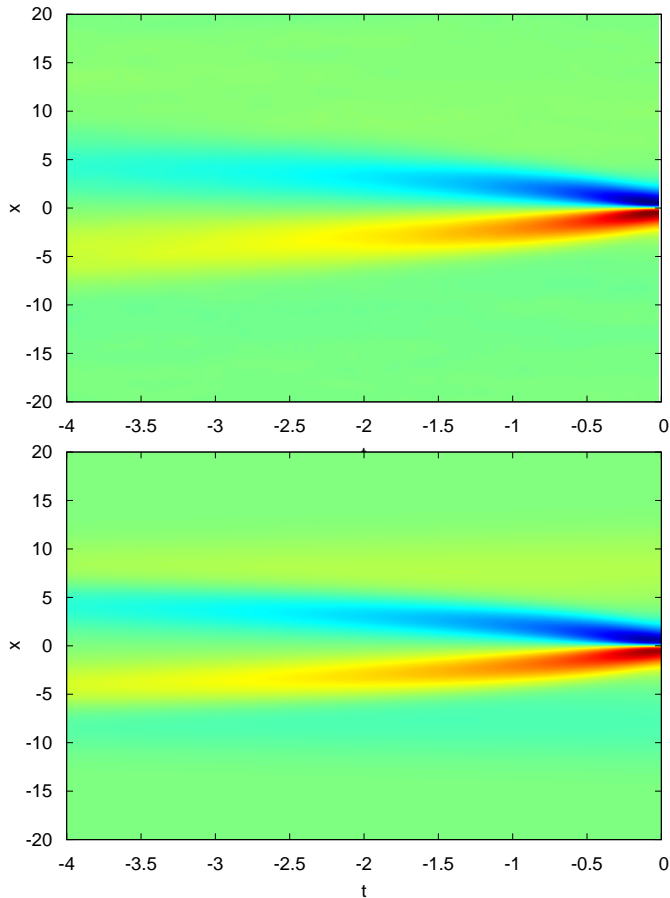


FIG. 2: Comparison of the filtered velocity field $\langle u_{\text{shifted}}(t, x) \rangle$ (top) and the instanton field $u(t, x)$ (bottom) as a space-time contour plot.

lations of the stochastic Burgers equation, we conducted the following numerical experiment: We started the integration of the stochastic Burgers equation from zero initial conditions for the velocity field $u(t = t_{\text{min}}, x) = 0$ at a large negative time t_{min} up to the final time $t = 0$. Typical parameters are summarized in table I. The initial time t_{min} was chosen corresponding to the instanton equations (6) and consists of more than 10 integral times T_L . This single experiment was repeated $\approx 10^7$ times using the 64 CUDA Tesla 1060 graphics on the Bochum

GPU Cluster and the 96 CUDA Fermi 2050 graphics cards on the CUNY GPU Cluster. The total simulation length obtained by this parallelism corresponds to $\approx 10^8$ integral times T_L . Each of these simulations was analyzed in the following way: We prescribed a small interval around a given value of the velocity gradient $u_x(t = 0, x) = a$ at the final time $t = 0$ and searched for the maximum velocity gradient in the numerical solution at that time. If we find that the maximum velocity gradient falls into the desired interval, we shift the field in space such that the location of the maximum velocity gradient is located at $x = 0$. In addition, we also shift the forcing field $\phi(t, x)$ in the same way. The averaging procedure now consists of taking the average of all those shifted fields $u_{\text{shifted}}(t, x)$ and $\phi_{\text{shifted}}(t, x)$. We thus obtain an ensemble average $\langle u_{\text{shifted}}(t, x) \rangle$ and $\langle \phi_{\text{shifted}}(t, x) \rangle$ in space and time. Since the forcing field is δ -correlated in time, it is obvious that in order to extract information of the averaged forcing field an enormous number of realizations is necessary. This numerical procedure now complies with the path integral formulation for the observable $\mathcal{O}(u) = \langle \delta(u_x(0, 0) = a) \rangle$

$$\langle \mathcal{O}(u) \rangle = \int \mathcal{D}f \mathcal{O}(u) \delta(u_t + uu_x - \nu u_{xx} - \phi) e^{-(\phi, \chi^{-1} \phi)/2} \quad (7)$$

which is the starting point for the Martin-Siggia-Rose formulation. Thus, for sufficiently strong velocity gradients $u_x(0, 0) = a$, the important question and conjecture is whether the averaged solutions $\langle u_{\text{shifted}}(t, x) \rangle$ and $\langle \phi_{\text{shifted}}(t, x) \rangle$ coincide with the instanton solution of (6). Especially if this conjecture is true, then the averaged optimal force $\langle \phi_{\text{shifted}}(t, x) \rangle$ should coincide with the right-hand side of equation (6a)

$$\langle \phi_{\text{shifted}}(t, x) \rangle = -i \int \chi(x - x') p(x', t) dx' \quad (8)$$

where the auxiliary field $p(t, x)$ is obtained from the direct Chernykh-Stepanov algorithm. Fig. (1) shows the filtered field $\langle u_{\text{shifted}}(t, x) \rangle$ (top) and the instanton field $u(t, x)$ (bottom) at the final time $t = 0$ and at an earlier time $t = -1.75$ showing the instanton in a different phase (see also the sketch of the instanton phases in Fig. 8 in [7]). The agreement is remarkable. Especially the center region is precisely reproduced by the stochastic simulation, while the sides are less pronounced. In order to get a complete overview of the time history of the instanton and the filtered field, Fig. (2) depicts a contour plot of the whole space-time domain. Although the filtered field shows a slightly shorter extent in time, the congruence is clearly visible.

The rareness of the filtered events has a strong impact on the agreement between the instanton approximation and the full stochastic simulation. In order to demonstrate the varying resemblance to the instanton approximation, we alter the probability of reaching a prescribed

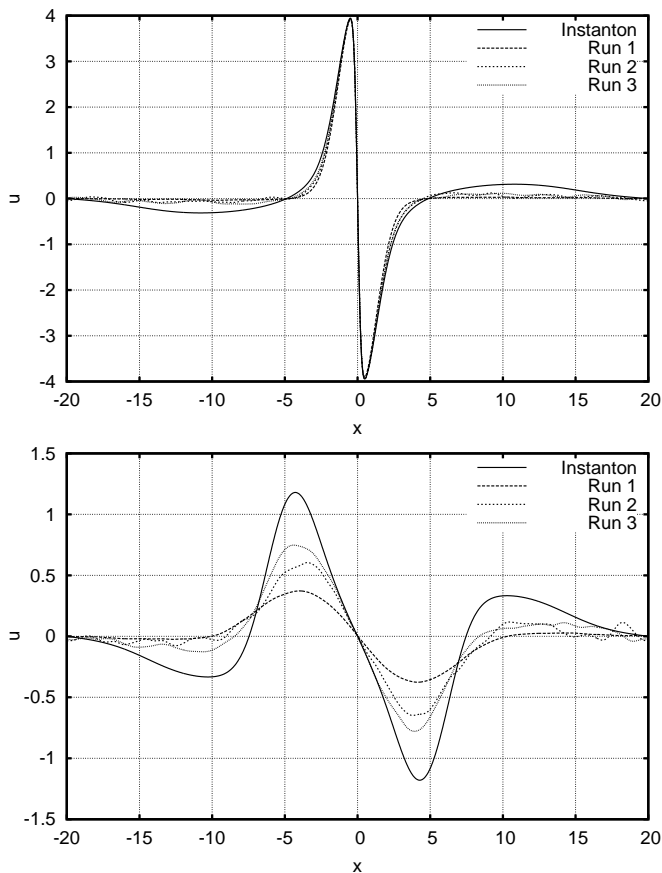


FIG. 3: Comparison of the instanton field $u(t, x)$ (solid) to stochastic simulations with varying hit percentages ($\approx 10\%$ (dashes), $\approx 0.5\%$ (dots), $\approx 0.05\%$ (small dots)) for $t = 0$ (top) and $t = -1.75$ (bottom). Agreement with the instanton approach increases with decreasing hit percentage.

velocity gradient by changing the kinematic viscosity ν . Fig. (3) shows the filtered field $\langle u_{\text{shifted}}(t, x) \rangle$ and the instanton field $u(t, x)$ for three different hit percentages. As the rareness of the event increases, accordance with the instanton grows considerably. Especially the velocity gradient in the origin is only reproduced when the events are rare. Notably this effect does not depend on the Reynolds number or shock strength, but on the scarcity of the event alone.

An additional feature of this filtering approach is that not only the instanton velocity field could be extracted but also the time history of the auxiliary field $p(t, x)$ and of the optimal force field. At time $t = 0$, the auxiliary field is given by its initial condition $p(t = 0, x) = -4i\nu^2 \mathcal{F} \delta'(x)$ and produces the force term $4\nu^2 \mathcal{F} \chi'(x)$ on the right-hand side of eqn. (6a). A comparison of this term with the filtered force field $\langle \phi_{\text{shifted}}(t, x) \rangle$ is depicted in Fig. (4), which shows a remarkable agreement.

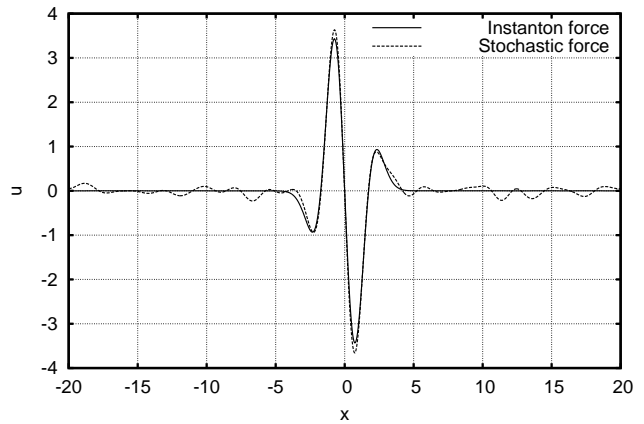


FIG. 4: The filtered force field $\langle \phi_{\text{shifted}}(t, x) \rangle$ (dashed) and the analytical force field $4\nu^2 \mathcal{F} \chi'(x)$ (solid) at time $t = 0$.

Conclusions and Outlook In this Letter we studied the question whether the instanton solution for Burgers turbulence is “real”, e.g. can be observed in stochastically driven simulations. The positive answer to this question is remarkable since we observe the instanton for a moderate Reynolds number and thus for moderate (and not extreme) values of the velocity gradient. In principle, this filtering method also allows a further study of moderately scarce events to determine where fluctuations around the instanton appear, how they look like and how they modify the action integral and thus the PDF. Our findings could also open the door to the issue why the PDF for the very left tail of velocity gradients could not be observed in high resolution numerical experiments of Gotoh [16]. Although this is out of the scope of the present Letter, work in this direction is in progress.

Acknowledgment We acknowledge stimulating discussion with M. Polyakov, R. Friedrich and M. Wilczek. Especially, we would like to thank M. Rieke for sharing his CUDA programming expertise. This work benefited from partial support through DFG-FOR1048 and the NSF grants DMS-0807396, DMS-1108780, and CNS-0855217. Numerical simulations were conducted on the CUDA-Cluster of the Research Department Plasma Physics at the Ruhr-University Bochum and the GPU-Cluster at the High Performance Computing Center of the City University of New York.

This paper is dedicated in memoriam of Professor Rudolf Friedrich (+16.8.2012).

-
- [1] B. Shraiman and E. Siggia, Phys. Rev. E **49**, 2912 (1994).
 - [2] V. Gurarie and A. Migdal, Phys. Rev. E **54**, 4908 (1996).
 - [3] G. Falkovich, I. Kolokolov, V. Lebedev, and A. Migdal,

- Phys. Rev. E **54**, 4896 (1996).
- [4] E. Balkovsky, G. Falkovich, I. Kolokolov, and V. Lebedev, Phys. Rev. Lett. **78**, 1452 (1997).
 - [5] E. Hopf, Comm. in Pure and Applied Math. **3**, 201 (1950).
 - [6] J. Cole, Quarterly Journal of Applied Mathematics **9**, 225 (1951).
 - [7] A. Chernykh and M. Stepanov, Phys. Rev. E **64**, 026306 (2001).
 - [8] P. C. Martin, E. D. Siggia, and H. A. Rose, Phys. Rev. A **8**, 423 (1973).
 - [9] H. Janssen, Z. Physik B **23**, 377 (1976).
 - [10] C. de Dominicis, J. Phys. C **1**, 247 (1976).
 - [11] R. Phythian, J. Phys. A **10** (1977).
 - [12] W. E., W. Ren, and E. van den Eijnden, Comm. Pure Appl. Math. **57**, 1 (2004).
 - [13] H. C. Fogedby and W. Ren, Phys. Rev. E **80**, 041116 (2009).
 - [14] H. Qi and D. Sun, SIAM J. Matrix Anal. Appl **28**, 360 (2006).
 - [15] A. Chekhlov and V. Yakhot, Phys. Rev. E **52**, 5681 (1995).
 - [16] T. Gotoh, Phys. Fluids **11**, 2143 (1999).